Adjusting the coherent transport in finite periodic superlattices

C. Pacher and E. Gornik
Institut für Festkörperelektronik und Mikrostrukturzentrum, Technische Universität Wien, 1040 Wien, Austria
(Received 11 March 2003; revised manuscript received 5 June 2003; published 21 October 2003)

The coherent transmission function and the tunneling time of one-dimensional arbitrary finite periodic structures are adjusted without changing the resonance energies and therefore the band positions. The method is based on modifications of the single period which are reflected in a similarity transformation of the corresponding transfer matrix. Applied to semiconductor superlattices a strong tuneable increase of the average miniband transmission is obtained. The maximum of the average miniband transmission is reached if the single period is built by a double barrier resonant tunneling diode. The fundamentally different transmission behavior compared to a standard superlattice is analyzed. Calculations of the phase tunneling time show that the increase of the transmission comes along with a faster tunneling process through the transmission resonances. All results are valid for any number of periods.

DOI: 10.1103/PhysRevB.68.155319 PACS number(s): 73.21.Cd, 73.21.Ac, 03.65.Xp

I. INTRODUCTION

In the past scattering and propagation of electromagnetic and quantum waves have been extensively studied. In solid-state physics the envelope function approximation (EFA)[1–5] made it possible to describe the periodic lattice potential of each layer by a material dependent effective electron mass m^* and a material dependent constant potential V. This powerful method together with the transfer matrix formalism[6,7] made the study of coherent transmission behavior of heterostructures very simple.

Finite periodic structures, in which each period consists of a barrier/well pair, called superlattices[8] (SL's) have been extensively examined[9–12,14] using the transfer matrix approach. The finiteness and periodicity are fully incorporated without any need for Bloch functions. The periodicity of a finite SL leads to resonances in the transmission function, where it reaches the maximum value of unity. Recently a comprehensive presentation, studying also multichannel systems, was given by Pereyra.[13]

In the present paper the effects of modifications of the unit cell of one-dimensional periodic structures, which are reflected in a similarity transformation of their transfer matrix, are studied. It is shown that the coherent transmission function and the tunneling time of arbitrary finite periodic structures can be adjusted without changing the resonance energies and therefore the band positions.

The paper is organized as follows. In Sec. II the established theory of transfer matrices, including the resonance conditions for finite periodic potentials, is briefly reviewed. Section III introduces the transformation of finite periodic potentials yielding an increase of the average transmission while keeping the resonance energies invariant. This transformation is applied to a SL in Sec. IV. We give analytical expressions for the transfer matrix and the transmission of the transformed SL's and show how the invariance of the resonance energies can be used to tune and optimize the transmission between the resonances in the minibands. In Sec. V the dependence of the integrated miniband transmission on the barrier width is studied for the modified SL's. Analytical approximations for the SL miniband width Δ and for the integrated transmission through the minibands of the modified SL's are given. Finally the phase tunneling times of the analyzed structures are calculated and discussed in Sec. VI. Numerical calculations for GaAs/AlGaAs SLs demonstrating the results complement Secs. IV to VI.

II. FINITE PERIODIC POTENTIALS

Here we will summarize mainly known results of one-channel transfer matrices for periodic potentials which we will use in the later sections. If we denote the one-dimensional wave function $\Psi(x)=A^+\exp(ikx)+A^-\exp(-ikx)$ of a region of constant potential as $\Psi=(A^+,A^-)^T$, the wave functions at the left and right interface of a certain region, Ψ_L and Ψ_R, respectively, are related by the transfer matrix M through[15] $(A_L^+,A_L^-)^T=M(A_R^+,A_R^-)^T$. Neglecting spin, the time reversal invariance and the conservation of the probability density current lead to the structure[17] of M

$$M=\begin{pmatrix} a & b \\ b^* & a^* \end{pmatrix}, \tag{1}$$

where

$$\det M=|a|^2-|b|^2=1, \tag{2}$$

$$\mathrm{Tr}(M)=a+a^*=2\,\mathrm{Re}\{a\} \tag{3}$$

holds.[17] In terms of the transmission and reflection coefficients t and r, the transfer matrix can be written as[12]

$$M=\begin{pmatrix} 1/t & r^*/t^* \\ r/t & 1/t^* \end{pmatrix}. \tag{4}$$

Since by construction the transfer matrix of a sequence of layers is the product of the transfer matrices of each layer, the transfer matrix of a potential consisting of n periods is the nth power of the transfer matrix of one period:

$$M^n=\begin{pmatrix} a^{(n)} & b^{(n)} \\ b^{(n)*} & a^{(n)*} \end{pmatrix}. \tag{5}$$

For $n \geqslant 2$, $a^{(n)}$ and $b^{(n)}$ can be expanded to[18]

$$a^{(n)} = a U_{n-1}(\mathrm{Re}\{a\}) - U_{n-2}(\mathrm{Re}\{a\}), \tag{6}$$

$$b^{(n)} = b U_{n-1}(\mathrm{Re}\{a\}), \tag{7}$$

where $U_n(x)$ denote the Chebyshev polynomials of the second kind. Using the recurrence relation $U_n(x) = 2x U_{n-1}(x) - U_{n-2}(x)$ and the relation $T_n(x) = U_n(x) - x U_{n-1}(x)$,[19] where $T_n(x)$ denote the Chebyshev polynomials of the first kind, we separate the real and the imaginary part of $a^{(n)}$, which correspond to the inphase and out of phase component of the inverse transmission coefficient, respectively:

$$\mathrm{Re}\{a^{(n)}\} = T_n(\mathrm{Re}\{a\}), \tag{8}$$

$$\mathrm{Im}\{a^{(n)}\} = \mathrm{Im}\{a\} U_{n-1}(\mathrm{Re}\{a\}). \tag{9}$$

It is interesting to note that the real part of the inverse transmission coefficient through any periodic structure is a function of the real part of one period only. The transmission $T^{(n)}$ of any (field-free) n-fold periodic structure is given by[10–13]

$$T^{(n)} = |a^{(n)}|^{-2} = [1 + |b|^2 U_{n-1}^2(\mathrm{Re}\{a\})]^{-1}. \tag{10}$$

Resonances with $T^{(n)} = 1$ occur if and only if $b^{(n)} = b U_{n-1}(\mathrm{Re}\{a\}) = 0$. Because $U_{n-1}(x)$ has $n-1$ zeros in $(-1,1)$ it can easily be seen that any n-fold periodic structure exhibits at least $n-1$ energy resonances where the transmission reaches exactly 1. Since $U_k(x) = 2^k \Pi_{i=1}^k [x - \cos i\pi/(k+1)]$ this yields[13,16]

$$T^{(n)} = 1 \Leftarrow \mathrm{Re}\{a\} = \cos(i\pi/n), \quad i = 1, \ldots, n-1. \tag{11}$$

Yuh and Wang[20] showed that the position of the minibands of *any infinite* periodic potential is given by the real solutions for q of the equation $\frac{1}{2}(M_{11} + M_{22}) = \cos qd$, where q is the Bloch wave vector and d is the length of one period. In our notation this reads

$$\mathrm{Re}\{a\} = \cos qd. \tag{12}$$

Equations (11) and (12) show directly the strong relation between energy resonances in finite periodic potentials and band positions in infinite periodic potentials. Identifying both cos arguments one finds the corresponding wave numbers[10] and wavelengths for the finite potential[16]

$$T^{(n)} = 1 \Leftarrow q_i = i\frac{\pi}{L} \Leftrightarrow \lambda_i = \frac{2\pi}{q_i} = \frac{2L}{i}, \tag{13}$$

where $L = nd$ is the length of the structure. This formulas show that the Bloch waves build standing waves across the entire periodic structure. The corresponding transmission resonances are Fabry-Pérot resonances.[16] Inserting the resonance condition Eq. (11) into Eq. (8) one easily verifies that $a^{(n)} = \pm 1$, indicating a 0 or π phase shift at resonance.

III. INVARIANCE OF RESONANCE ENERGIES-INCREASE OF TRANSMISSION

In this section we show the first important result of this paper: a method which increases the coherent transmission of periodic structures without changing the miniband positions and even the individual resonance energies inside the minibands. Since the envelope of the maxima of $U_{n-1}^2(x)$ for $|x| \leqslant 1$ is given by $1/(1-x^2)$, from Eq. (10) follows that the envelope of the minima of $T^{(n)}$ is given by

$$T_{\min} = \left[1 + \frac{|b|^2}{1 - \mathrm{Re}^2\{a\}}\right]^{-1}. \tag{14}$$

The transmission $T^{(n)}$ is bounded below by $T_{\min}$ and above by unity for any arbitrary number n of periods. Therefore our results are valid for arbitrary number of periods, even in the limit $n \to \infty$. Equation (14) together with (11) yields that for a fixed $\mathrm{Re}\{a\}$ a change of $|b|$ would only change the transmission between the resonance peaks but not their position. To achieve this we apply a similarity transformation to the transfer matrix M of a single cell of the periodic potential

$$M' = M_1^{-1} M M_1. \tag{15}$$

Since the trace of a matrix is invariant under a similarity transformation, i.e., $\mathrm{Tr}\{M'\} = \mathrm{Tr}\{M\}$, this yields the desired result

$$\mathrm{Re}\{a'\} = \mathrm{Re}\{a\}, \tag{16}$$

while in general $|b'| \neq |b|$. If the transfer matrix M is written as the product of two matrices it is easy to see how this similarity transformation can be performed:

$$M = M_1 M_2 \Rightarrow M' = M_1^{-1} M M_1 = M_2 M_1. \tag{17}$$

In terms of the corresponding potentials $V(x), V'(x)$, $V_1(x)$, and $V_2(x)$, which belong to the transfer matrices M, M', M_1, and M_2, respectively, this reads

$$V(x) = \{V_1(x); V_2(x)\},$$

$$V'(x) = \{V_2(x); V_1(x)\}, \tag{18}$$

where $\{\cdots;\cdots\}$ denotes the concatenation of two potentials. $V'(x)$ is the potential which results from $V(x)$ by shifting a part, namely, $V_1(x)$, from the left to the right side. Different partitions of $V(x)$ into $V_1(x)$ and $V_2(x)$ lead to different $V'(x)$, and therefore in general to different $|b'|$ and consequently to different transmission values between the fixed resonance positions. Thus for an optimization of the transmission between the energy resonances one has to find the optimal partition of $V(x)$ or, in other words, the optimal dividing point of the unit cell.

From the power of the transfer matrix M'

$$M'^n = (M_1^{-1} M M_1)^n = M_1^{-1} M^n M_1 \tag{19}$$

it can be seen that the similarity transformation given in Eq. (15) also belongs to finite periodic sequences of $V(x)$ and $V'(x)$, i.e., to $\{V(x)\}^n$ and $\{V'(x)\}^n$. Writing Eq. (19) in the form $M'^n = M_2 M^{n-1} M_1$, we see that only the interfaces to the environment are changed. Inside the structure $n-1$ periods remain unchanged.

If we divide the finite periodic sequence $\{V(x)\}^n$ at an arbitrary position in a left and right part, namely, $V_L(x)$ and

TABLE I. Variables and functions used.

L_b	barrier thickness
L_w	well thickness
m_b	effective electron mass in the barriers (Ref. 23)
m_w	effective electron mass in the wells (Ref. 23)
V_b	potential energy of barriers
E	energy
$k=k(E)=(2m_wE)^{1/2}/\hbar$	electron wave vector in the wells
$\kappa=\kappa(E)=[2m_b(V_b-E)]^{1/2}/\hbar$	decaying electron wave vector in the barriers
$c_1=c_1(E)=\frac{1}{2}\left(\frac{k}{\kappa}\frac{m_b}{m_w}+\frac{\kappa}{k}\frac{m_w}{m_b}\right)$	
$c_2=c_2(E)=\frac{1}{2}\left(\frac{k}{\kappa}\frac{m_b}{m_w}-\frac{\kappa}{k}\frac{m_w}{m_b}\right)$	

$V_R(x)$, we can define the corresponding transfer matrices $M_L:=M^pM_1, M_R:=M_1^{-1}M^{n-p}$ $(p\in\mathbb{N}, 0\leqslant p<n)$, where p is the number of complete periods in $V_L(x)$ and M_1 corresponds to the left part of the divided period. Since $M^n=M_LM_R$ and $M'^n=M_RM_L$ this proves that the resonance energies are invariant if we divide a finite periodic potential at an arbitrary position into two parts and reverse the order of them.[22]

Periodic sequences of the form $\{V_1(x);V_2(x);\cdots;V_k(x)\}^n$ show exactly the same behavior under cyclic permutations, since $[(M_1M_2\cdots M_l)(M_{l+1}\cdots M_k)]^n$ transforms to $[(M_{l+1}\cdots M_k)(M_1M_2\cdots M_l)]^n$.

IV. SUPERLATTICES

In the following we apply the results of the previous section to the simplest case, a SL with n periods, alternatively consisting of barriers (B) and wells (A) and show that the average transmission can be increased without changing the resonance positions. All variables and functions which are used from now on are summarized in Table I.

A. $(BA)^n$ superlattices

For the sake of completeness we will very briefly derive the well known transmission for a normal SL with n periods. For one period of a normal SL we get $M_{\mathrm{SL}}^{(1)}=M_BM_A$, where M_B and M_A are the transfer matrices for a barrier and a well, respectively. Formulas for M_A, M_B, and $M_{\mathrm{SL}}^{(1)}$ are given by Eqs. (A1), (A2), and (A3) in the appendix. The transmission $T_{\mathrm{SL}}^{(n)}$ of the SL with n periods follows from Eq. (10):[10–13]

$$T_{\mathrm{SL}}^{(n)}=[1+|b_{\mathrm{SL}}^{(1)}|^2U_{n-1}^2(\mathrm{Re}\{a_{\mathrm{SL}}^{(1)}\})]^{-1}$$

$$=\frac{1}{1+\{A(L_b)U_{n-1}[P(L_b)]\}^2}, \tag{20}$$

where we introduced

$$A(L_b)=|b_{SL}^{(1)}|=c_1\sinh\kappa L_b, \tag{21}$$

$$P(L_b)=\mathrm{Re}\{a_{SL}^{(1)}\}=\cosh\kappa L_b\cos kL_w-c_2\sinh\kappa L_b\sin kL_w. \tag{22}$$

B. $(B^{1-\gamma}AB^{\gamma})^n$ superlattices

We start from the unit cell BA of a SL and define in the face of Eq. (18) $V_1(x)$ to be a part of the barrier B^{γ} and $V_2(x)$ to be the rest of the period $B^{1-\gamma}A$. If we change the order, according to Eq. (18), to $\{V_2(x),V_1(x)\}$, we get the structure $B_1AB_2=B^{1-\gamma}AB^{\gamma}$ $(0\leqslant\gamma\leqslant1)$. Now the period is built by an asymmetric resonant tunneling diode (ARTD), for which the sum of the widths of the barriers $B^{1-\gamma}$ and B^{γ} equals the width of the original SL barriers $B[L_{b1}=(1-\gamma)L_b, L_{b2}=\gamma L_b]$. Since $(B^{1-\gamma}AB^{\gamma})^n=B^{1-\gamma}(AB)^{n-1}AB^{\gamma}$, a periodic sequence of these ARTD's, results again in a structure very similar to the normal SL (Fig. 1), only the outmost barriers are modified. From Eq. (16) we know that $\mathrm{Re}\{a_{B1AB2}\}=\mathrm{Re}\{a_{\mathrm{SL}}^{(1)}\}$. Equations (11) and (12) show that the real part of a exclusively defines the resonance energies and the miniband positions. Therefore $(B^{1-\gamma}AB^{\gamma})^n$-SL's possess all resonance energies of normal $(BA)^n$-SL's and also the miniband positions are equal. The beneficial effect of the modification from $(BA)^n$ to $(B^{1-\gamma}AB^{\gamma})^n$ can be seen in the transmission. We calculate $|b|$ of the structure B_1AB_2 and then make use of Eq. (10). The calculation of b leads to

$$b_{B1AB2}=2iA(L_b/2)P(L_b/2)-2A(\Delta L_b/2)[\cosh(\kappa\Delta L_b/2)$$
$$-ic_2\sinh(\kappa\Delta L_b/2)]\sin kL_w, \tag{23}$$

where $\Delta L_b=L_{b1}-L_{b2}=(1-2\gamma)L_b$. To complete the transfer matrix, $\mathrm{Im}\{a_{B1AB2}\}$ is given by Eq. (A5). The transmission through a $(B^{1-\gamma}AB^{\gamma})^n$-SL is given by

$$T_{B1AB2}^{(n)}=\{1+|b_{B1AB2}|^2U_{n-1}^2[P(L_b)]\}^{-1}. \tag{24}$$

For energies E_j^* at which $\sin k_j^*L_w=0$ is fulfilled, b_{B1AB2} does not depend on ΔL_b. At these energies all structures behave as n successive barriers. Equation (22) reduces to $P(L_b)=\cosh\kappa L_b$. Since $\cosh\kappa L_b>1$ $(\cosh\kappa L_b<1)$ for $E<V_b$ $(E>V_b)$, these energies E_j^* are in the minigaps (minibands) where $|P(L_b)|>1$ $(|P(L_b)|<1)$. Applying Eq. (14) leads to

$$T_{\min}=\left[1+\frac{|b_{B1AB2}|^2}{1-P^2(L_b)}\right]^{-1}. \tag{25}$$

Since for $E\neq E_j^*$ the term $|b_{B1AB2}|^2$ depends strongly on ΔL_b it is possible to tune the transmission between the energy resonances in a wide range by choosing a proper ΔL_b. Since the number of periods only influences the transmission above $T_{\min}$, this general behavior also persists when $n\to\infty$.

C. Superlattices with antireflection coating $(B^{1/2}AB^{1/2})^n$

Following the statement in Sec. III, we have to find the optimal partition of the single SL cell, i.e., the optimal value of ΔL_b, to get the optimal miniband transmission. From the calculation of the derivative of $|b_{B1AB2}|^2$ with respect to ΔL_b

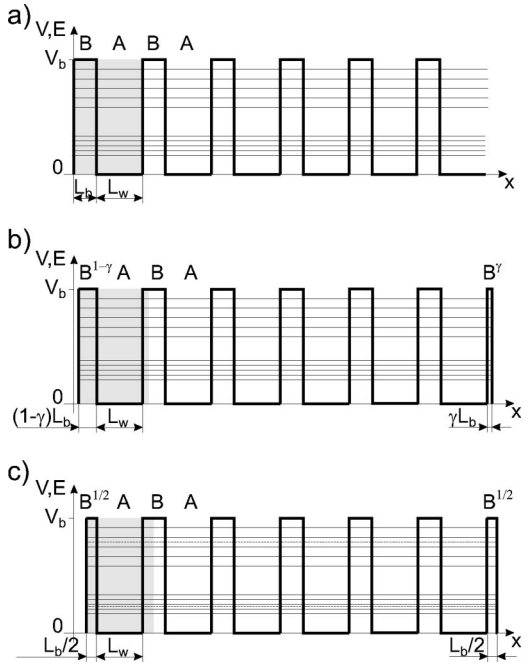

FIG. 1. Schematic potential of (a) normal SL of the form $(BA)^n$, (b) SL of the form $(B^{1-\gamma}AB^{\gamma})^n$ with $0 \leqslant \gamma \leqslant 1/2$, and (c) SL of the form $(B^{1/2}AB^{1/2})^n$, also called an SL with antireflection coating (ARC). The number of periods n is chosen to be 6. The shaded regions mark one period of each potential. All three structures have the same $n-1=5$ Fabry-Pérot energy resonances in each miniband, indicated by thin solid horizontal lines. The structure $(B^{1/2}AB^{1/2})^n$ possesses one additional resonance per miniband, marked by thin dashed lines.

(explicitly done in Appendix B) and Eq. (24), we see that for $E<V_b$ the transmission Eq. (24) is strictly monotonic increasing with decreasing ΔL_b and reaches a maximum for $\Delta L_b=0$. In this special case the basis of the periodic potential is built by a symmetric resonant tunneling diode (symmetric RTD) with a barrier width of $L_b/2$.

Therefore a SL of the form $(B^{1/2}AB^{1/2})^n$ has the maximum average transmission and a normal SL of the form $(BA)^n$ has the minimum average transmission of all structures of the form $(B^{1-\gamma}AB^{\gamma})^n$ for energies below the barrier height V_b. In Appendix B we show that this strict monotony does not persist for energies above the barriers [as can be seen in Fig. 2(c) for the third miniband], i.e., that there are energy intervals where the antireflection coating reduces the transmission.

The $(B^{1/2}AB^{1/2})^n$ structure can be seen as a normal SL between an anti reflection coating (ARC).[16] Equation (23) then reduces to

$$b_{B/2AB/2}=2iA(L_b/2)P(L_b/2), \tag{26}$$

and the transmission is given by[16]

$$T^{(n)}_{\mathrm{SLARC}}=\frac{1}{1+\{2A(L_b/2)P(L_b/2)U_{n-1}[P(L_b)]\}^2}. \tag{27}$$

The additional term $P(L_b/2)$ in the denominator of Eq. (27) compared to Eq. (20) gives rise to one additional transmission resonance $\hat{E}_i$ within each miniband. These resonances at $\hat{E}_i$ are the transmission resonances of the symmetric RTD $B^{1/2}AB^{1/2}$, which of course appear in a periodic sequence. Comparing $P(L_b/2)=0$ with $P(L_b/2)=\cos(qd)$, we find that this happens at $q=\pi/2d$, which leads to $d=\lambda/4$. At $\hat{E}_i$ the half width barriers act as a $\lambda/4$ layer similar to a $\lambda/4$-anti reflection layer in optics.[16]

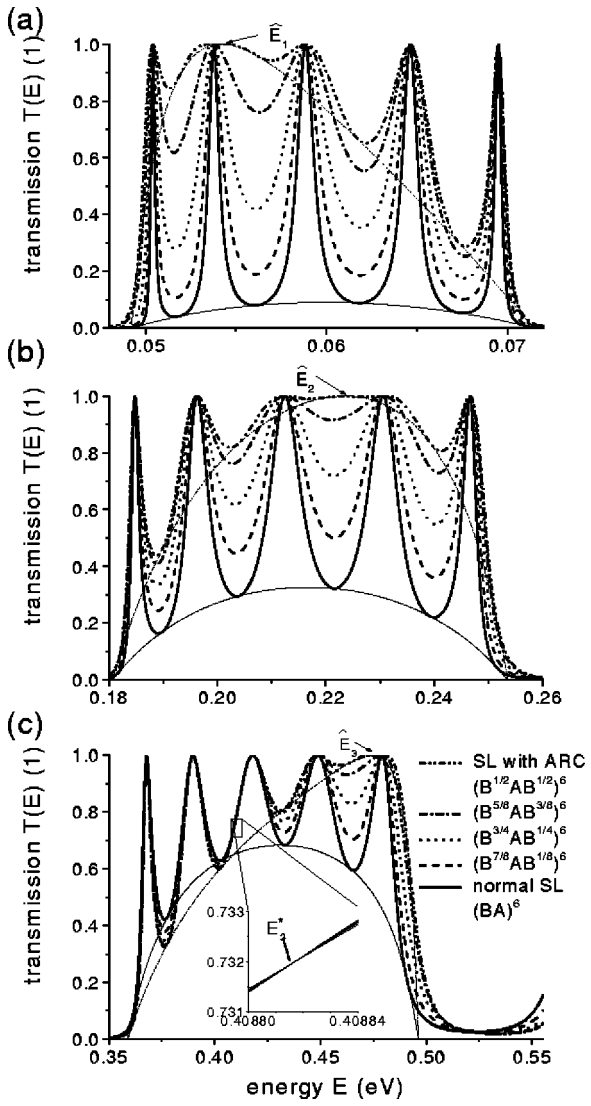

FIG. 2. Calculated transmission (thick lines) of the first three minibands, Eq. (24), of $GaAs/Al_{0.3}Ga_{0.7}As$ SL structures (barrier width $L_b=2.5$ nm, well width $L_w=6.5$ nm, further material parameters are given in the text) of the form $(B^{1-\gamma}AB^{\gamma})^6$ for $\gamma \in \{0,1/8,\ 1/4,\ 3/8,1/2\}$. The positions of the transmission resonances in all minibands do not depend on γ. (a) and (b) Demonstrate that a monotone behavior for all energies is observed for the first and the second miniband which are in the bandgap of the AlGaAs barriers. (c) Shows that the monotone behavior does not persist for minibands above the barriers. The envelopes of the transmission minima (thin lines) are additionally plotted for the $(BA)^6$ and $(B^{1/2}AB^{1/2})^6$ structures (shown for all structures in Fig. 3). $\hat{E}_1$, $\hat{E}_2$, and $\hat{E}_3$ mark the additional resonances in the $(B^{1/2}AB^{1/2})^6$ structure. E_3^* mark the energy at which the transmission is independent from γ.

D. Calculation for GaAs/$Al_{0.3}Ga_{0.7}As$ superlattices

To demonstrate the studied behavior we show in Fig. 2 the transmission $T^{(n)}_{B1AB2}$ of SL's ($n=6$) consisting of $Al_{0.3}Ga_{0.7}As$ barriers with $L_b=2.5$ nm and GaAs wells with $L_w=6.5$ nm. We plot the transmission for five different values of γ (or ΔL_b) as a function of energy for the first, second, and third miniband. The calculations are performed for the Γ valley of the conduction band for a temperature of 4 K using the following material parameters: (i) band edge effective masses as a function of Al content x: $m_e(x)=(0.067+0.0838x)m_0$, (ii) nonparabolicity of the conduction bands: $m_w=m(0,E)$, $m_b=m(x,E)$ with $m(x,E)=m_e(x)[1+(E-V)/0.7E_g(x)]$, where $E_g(x)=(1.512+1.455x)$ eV is the band gap, and (iii) conduction band offset: $V_b=0.66[E_g(x)-E_g(0)]=288.09$ meV. A schematic of the conduction band is drawn in Fig. 1. In Figs. 2(a) and 2(b) one can see the monotone relation between γ (or ΔL_b) and the transmission for the first and the second miniband, which are both below the potential of the barriers. This behavior has already been discussed in the previous section and proved in Appendix B in Eqs. (B2) and (B5). In Fig. 2(c) the transmission for the third miniband, which is above the barriers, is shown. The transmission resonances again do not depend on γ, but below an energy of $E_3^*\approx 409$ meV we observe a completely inverted behavior compared to the minibands below the barriers: the transmission increases monotonic with decreasing γ, and reaches its maximum for the normal SL structure. At E_3^* the transmission does not depend on γ, and above E_3^* (but only inside the third miniband) the same monotone behavior as for the first and second miniband is observed.

Figure 3 shows the envelope of the transmission minima $T_{\min}$ for $\gamma\in\{0,1/8,1/4,3/8,1/2\}$ for the first three minibands. As already pointed out, the transmission is bounded below by $T_{\min}$ and above by unity for any arbitrary number n of periods. Therefore our results are valid for arbitrary number of periods, even in the limit $n\to\infty$.

V. INTEGRATED MINIBAND TRANSMISSION

In this section the influence of the ratio γ on the transmission of the SL minibands is studied while varying additionally the barrier width L_b. To motivate this study Fig. 4 shows the calculated transmission of the first miniband on a logarithmic scale for a constant well width of $L_w=6.5$ nm and three different values of L_b (2.5, 6, and 8 nm). The increasing effect of the modifications ($\gamma\neq 0$) of the SL's can be seen by considering the values of the transmission function between the resonances. For the thickest barriers (8 nm) the difference between the standard SL and the SL with ARC is by a factor of about 10^4. Further it is interesting to note that the transmission shape for the SL with ARC is not changed at all. The only difference between the three $(B^{1/2}AB^{1/2})^6$ structures with different L_b's is the change of the miniband width. This shows that the transmission behavior can be fundamentally changed by the modification introduced in Sec. III.

A. Numerical integration

Since it is not possible to analytically integrate the transmission of any SL structure presented here, we started with a numerical integration of the transmission of the first miniband

$$T^1_{\text{int}}=\int_{E^1_{\min}}^{E^1_{\max}} T(E)dE.$$

$E^1_{\max}$ and $E^1_{\min}$ denote the upper and the lower edge of the first miniband, given by $P(L_b)=\mp 1$. The transmission $T(E)$ is given by Eq. (24). We note that the integrated transmission T^1_{int} does not essentially depend on the number of periods n provided that $n\gg 1$. In our case the relative difference between 6 and 7 periods for $L_b=2$ nm is 6×10^{-4}. The parameters for the SL's are the same that we used for Figs. 2 to 4 except that the width of the barriers L_b is varied between 1 and 8 nm. Comparing SL's ($L_b=8$ nm, $L_w=6.5$ nm) with $\gamma=0$ and $\gamma=1/2$, the integrated transmission is enhanced by a factor of more than 100. For $\exp(-\kappa L_b)\ll 1$, Fig. 5 shows an exponential relation between T^1_{int} and the barrier width L_b for all values of γ. The calculated miniband width is additionally plotted and its relation to the integrated miniband transmission is discussed at the end of this section. The modulus of the negative exponent has its maximum (1.3557) for the case of the normal SL ($\gamma=0$) and decreases with increasing γ, reaching its minimum (0.6785) for $\gamma=1/2$. The ratio of the maximum and minimum exponent is $2-1.9\times 10^{-4}$. To gain more insight into this interesting behavior we approximate the transmission expression in order to perform analytical integration.

B. Analytic approximations for $(BA)^n$ superlattices

From the transmission for a periodic structure, given by Eq. (10) and for the SL case by Eq. (20), we calculate the full width at half maximum (FWHM) of the single resonances. To make sure that we have at least one resonance we assume that the number of periods n is at least 2. For $T^{(n)}=1/2$, the condition

$$|bU_{n-1}[P(L_b)]|=1 \tag{28}$$

has to be fulfilled. Expanding $U_{n-1}[P(L_b)]$ around the ith resonance energy, where $P(L_b)=\cos i\pi/n$, into its Taylor series of first order, leads to

$$|U_{n-1}[P(L_b)+\Delta P(L_b)]|\approx \frac{n}{\sin^2\dfrac{i\pi}{n}}\,|\Delta P(L_b)|. \tag{29}$$

For $\kappa L_b\gg 1$ we can replace the hyperbolic functions in Eq. (22) by exponential functions. Further we will approximate $f(E):=\cos kL_w-c_2\sin kL_w$ in the energy range where $|P(L_b)|\leqslant 1$ (inside the jth miniband) by its Taylor series of first order around the center energy E_0^j of the jth miniband, leading to

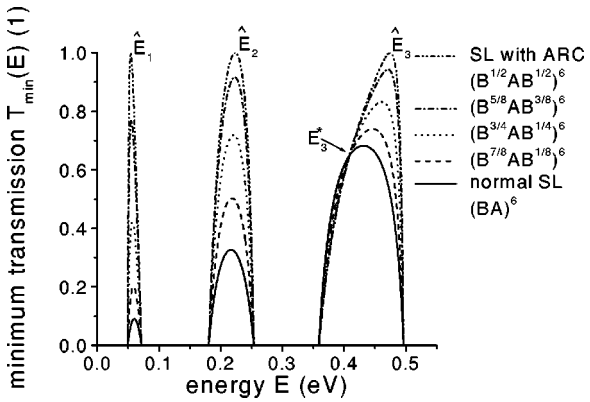

FIG. 3. Calculated envelope of the transmission minima by Eq. (25), corresponding to the transmission functions plotted in Fig. 2.

$$P(L_b)\approx \frac{f_j'}{2}(E-E_0^j)\exp \kappa L_b, \quad f_j'=\frac{df(E)}{dE}(E_0^j). \quad (30)$$

E_0^j is given by the jth solution of the equation $f(E)=0$ and is also the solution of the jth bound state of an isolated quantum well of thickness L_w. Changing the energy from the ith resonance in the jth miniband E_i^j to the value $E_i^j+\Delta E_i^j/2$, where the transmission $T^{(n)}$ has dropped to 1/2, the corresponding change in $P(L_b)$ is given by

$$\Delta P(L_b)\approx \frac{1}{2}f_j'\frac{\Delta E_i^j}{2}\exp \kappa L_b. \quad (31)$$

Substituting Eq. (31) into Eq. (29), together with Eq. (28) yields

$$\Delta E_i^j\approx \frac{4\sin^2\frac{i\pi}{n}}{n|f_j'||b|}\exp(-\kappa L_b). \quad (32)$$

Up to this point all results in this section are only restricted to structures with well separated resonances, but no further restrictions are necessary. Now we concentrate on $(BA)^n$-SL's. Using $|b_{\mathrm{SL}}^{(1)}|=c_1\sinh \kappa L_b\approx(c_1/2)\exp \kappa L_b$, where c_1 is evaluated at the center E_0^j of the miniband, this gives the FWHM for the ith resonance in the jth miniband:

$$\Delta E_i^j\approx \frac{8\sin^2\frac{i\pi}{n}}{nc_1|f_j'|}\exp(-2\kappa L_b). \quad (33)$$

In the framework of the above Taylor series expansion of $U_{n-1}[P(L_b)]$ the SL transmission resonances are Lorentz curves of the form

$$\tilde{T}_{i,\mathrm{SL}}^{j(n)}(E)=\left[1+\left(\frac{E-E_i^j}{\Delta E_i^j/2}\right)^2\right]^{-1}. \quad (34)$$

Integrating and summing over all n resonances of the miniband finally leads to the approximated integrated transmission of the jth miniband

$$\tilde{T}_{\mathrm{SL\,int}}^{j}=\sum_{i=1}^{n-1}\int_{j\text{th res}}\tilde{T}_{i,\mathrm{SL}}^{j(n)}(E)dE=\frac{2\pi}{c_1|f_j'|}\exp(-2\kappa L_b). \quad (35)$$

In agreement with our comment from section V-A $\tilde{T}_{\mathrm{SL\,int}}^{j}$ does not depend on the number of periods n. If one applies above calculations to the case $n=2$, where the potential forms a symmetric RTD, Eq. (29) holds exact and one ends again with

$$\tilde{T}_{\mathrm{RTD\,int}}^{j}=\int_{j\text{th res}}T_{1,\mathrm{SL}}^{j(2)}dE=\frac{2\pi}{c_1|f_j'|}\exp(-2\kappa L_b). \quad (36)$$

This shows that the integrated transmission through the jth miniband of a SL with an arbitrary number of periods n is equal to the integrated transmission through the jth resonance of a symmetric RTD with the same barrier and well

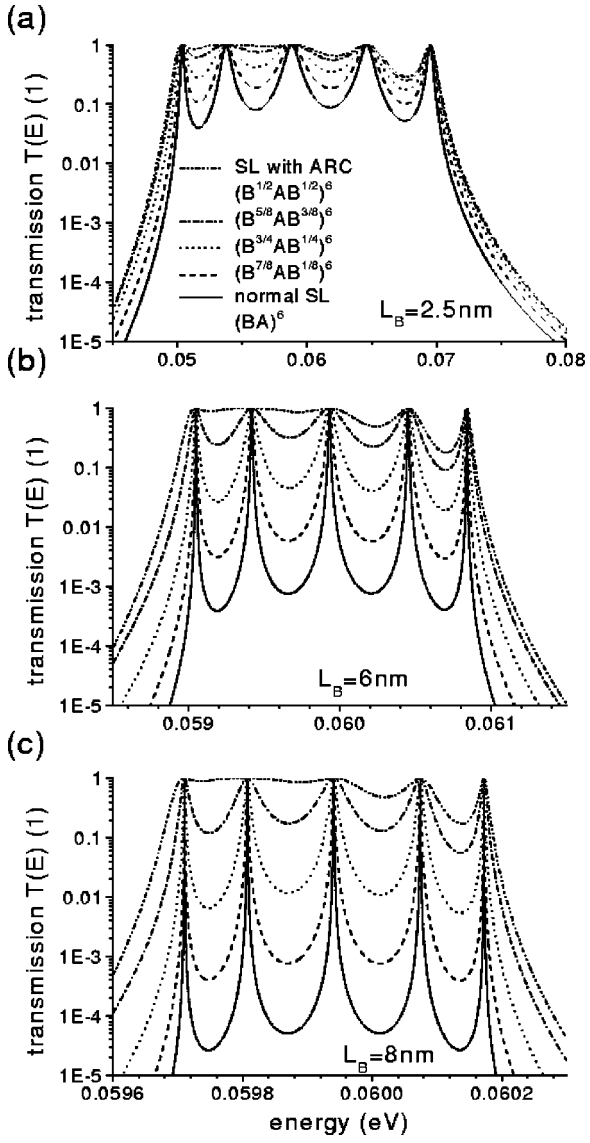

FIG. 4. Transmission of the first miniband of $(B^{1-\gamma}AB^{\gamma})^6$ structures for a barrier width L_b of (a) 2.5 nm, (b) 6 nm, and (c) 8 nm. The well width L_w is 6.5 nm for all three structures.

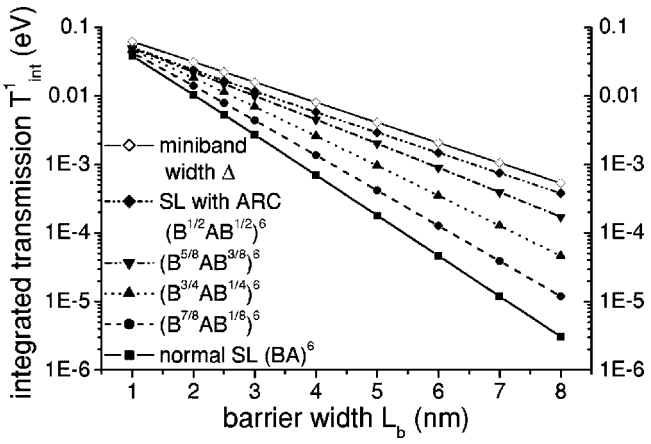

FIG. 5. Numerically integrated transmission of the first miniband of $(B^{1-\gamma}AB^{\gamma})^6$ structures as a function of the barrier width L_b. The open diamonds show as a comparison the width of the miniband.

width as the SL. The only condition is that the resonances are well approximated by a Lorentzian. In terms of ballistic current both structures behave similar given that the 1D electron distribution function is constant throughout the miniband width.

Making use of Eq. (30), the boundaries of the jth miniband, $E^j_{\max}$ and $E^j_{\min}$, respectively, are given by $\frac{1}{2}|f_j'|(E^j_{\max/\min}-E^j_0)\exp\kappa L_b=\pm 1$. The width Δ_j of the miniband then reads

$$\Delta_j=E^j_{\max}-E^j_{\min}=\frac{4}{|f_j'|}\exp(-\kappa L_b). \tag{37}$$

If we compare Eqs. (35) and (37) we notice that *the integrated miniband transmission* $\tilde{T}^j_{\mathrm{SL\,int}}$ *is not proportional to the miniband width* Δ_j, i.e., the ratio

$$\tilde{T}^j_{\mathrm{SL\,int}}/\Delta_j\sim\exp(-\kappa L_b) \tag{38}$$

decreases exponentially with increasing L_b.

C. Analytic approximations for $(B^{1/2}AB^{1/2})^n$ superlattices

Since the transmission resonances are not well separated for the SL with ARC, a different approach for the integration is used. The integral of the transmission of the SL with ARC is mainly given by the integral of $T_{\min}$, Eqs. (25) and (26). Since this curve is concave and reaches a point where $T=1$, the following inequality holds:

$$\begin{aligned}\frac{\Delta_j}{2}&=\frac{2}{|f_j'|}\exp(-\kappa L_b)\\&<\int_{j\text{th miniband}}T^{(n)}_{\mathrm{SLARC}}dE\\&<\frac{4}{|f_j'|}\exp(-\kappa L_b)=\Delta_j.\end{aligned} \tag{39}$$

TABLE II. Dependency of important miniband parameters as a function of the barrier width L_b.

	$(BA)^n$	$(B^{1/2}AB^{1/2})^n$
FWHM ΔE, Eq. (33)	$\exp(-2\kappa L_b)$	—
integrated miniband transmission $T^{(n)}_{\mathrm{int}}$, $n\geqslant 2$ Eqs. (35), (39)	$\exp(-2\kappa L_b)$	$\exp(-\kappa L_b)$
miniband width Δ, Eq. (37)	$\exp(-\kappa L_b)$	$\exp(-\kappa L_b)$

Therefore the integrated miniband transmission of a SL *with* ARC *is of the same order as the miniband width,* i.e.,

$$\frac{1}{2}<T^j_{\mathrm{SLARC\,int}}/\Delta_j<1, \tag{40}$$

in contrast to the behavior of a normal SL, as stated in Eq. (38). This phenomenon can be seen in Fig. 5 and is the second important result of this paper. Table II summarizes the results of this section.

VI. TUNNELING TIMES

We proceed by showing that the increase of the off-resonance transmission in $(B^{1-\gamma}AB^{\gamma})^n$-SL's, which we studied in the previous section, comes along with a decrease of the in-resonance phase tunneling time. Recently the concept of the phase tunneling time was successfully applied by Pereyra, who showed results in good agreement with optical-pulse tunneling experiments in the gap of periodic structures.[21] Given the transmission coefficient $t_V=|t_V|\exp(i\phi_V)$ of any arbitrary potential V, the phase time is defined to be $\tau_V=\partial\phi_V/\partial\omega$. If we use the inverse transmission coefficient $a_V=t_V^{-1}$ the phase time can be written in terms of the real and imaginary part of a_V:

$$\tau_V=-\hbar\frac{\partial}{\partial E}\arctan\frac{\mathrm{Im}\{a_V\}}{\mathrm{Re}\{a_V\}}. \tag{41}$$

For an n-fold periodic structure we replace a_V by $a^{(n)}$, use Eqs. (8) and (9) and get after some algebra

$$\begin{aligned}\tau^{(n)}=\hbar T^{(n)}\Bigg[&\left(n-\frac{\mathrm{Re}\{a\}}{2}U_{2n-1}(\mathrm{Re}\{a\})\right)\\&\times\frac{\mathrm{Im}\{a\}}{1-\mathrm{Re}^2\{a\}}\frac{\partial\mathrm{Re}\{a\}}{\partial E}\\&-\frac{1}{2}U_{2n-1}(\mathrm{Re}\{a\})\frac{\partial\mathrm{Im}\{a\}}{\partial E}\Bigg],\end{aligned} \tag{42}$$

where $T^{(n)}$ is the transmission probability of the periodic structure given by Eq. (10). This result is simpler than the one obtained in Ref. 21.

Using Eqs. (22) and (A5) we plot in Fig. 6 the tunneling times as a function of the energy for the $(B^{1-\gamma}AB^{\gamma})^n$-SL's studied in Sec. IV D. The resonant behavior of the transmission probability $T^{(n)}$ is reproduced also in the tunneling time characteristic: the maxima of the tunneling time are almost at the energy positions of the transmission maxima. The tunneling time peak values depend strongly on the position of the

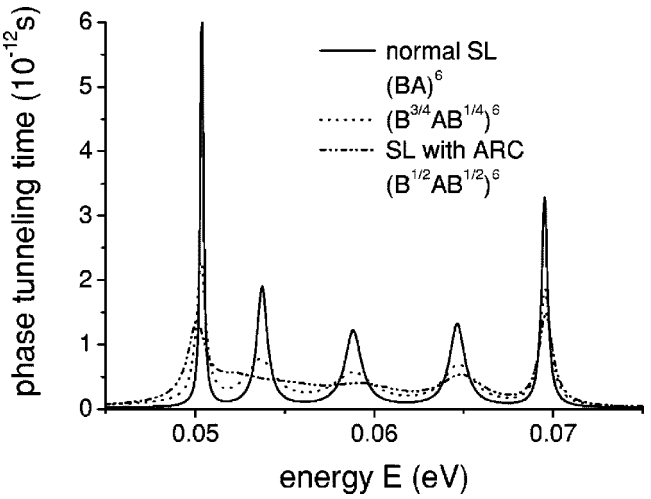

FIG. 6. Calculated phase tunneling time through $GaAs/Al_{0.3}Ga_{0.7}As$ SL structures of the form $(BA)^6$,$(B^{3/4}AB^{1/4})^6$, and $(B^{1/2}AB^{1/2})^6$ in the range of the first miniband.

resonances in the miniband: the outmost resonances possess the highest tunneling times, near the middle of the miniband the in-resonance tunneling time reaches its minimum. Since the widths of the transmission resonance peaks show the inverse behavior this is in complete agreement with the energy-time uncertainty relation.

If we compare $(B^{1-\gamma}AB^{\gamma})^n$-SL's with increasing values of γ up to 1/2, we observe a strong, monotone decrease of the in-resonance tunneling time. (For clarity reasons only three curves are drawn in Fig. 6.) Equation (42) allows us to calculate the tunneling time at resonance analytically. From the transmission resonance condition $T^{(n)}=1$, Eq. (11), follows directly $U_{2n-1}(\mathrm{Re}\{a\})=0$, which reduces Eq. (42) to

$$\tau_{\mathrm{res}}^{(n)}=\hbar n\frac{\mathrm{Im}\{a\}}{1-\mathrm{Re}^2\{a\}}\frac{\partial \mathrm{Re}\{a\}}{\partial E}. \tag{43}$$

This equation is universal for any periodic structure. The number of periods n enters only as a factor. Therefore the following conclusions of Eq. (43) are again valid for all n. Applied to $(B^{1-\gamma}AB^{\gamma})^n$-SL's, the dependence of $\mathrm{Im}\{a\}$ on γ makes it possible to adjust the in-resonance tunneling time in a certain range by choosing a proper value of γ. With Eq. (A5) and the fact that $\sin(kL_w)$ and $\partial\,\mathrm{Re}\{a\}/\partial E$ both change their signs between the minibands we directly proof that

$$\frac{\partial \tau_{\mathrm{res}}^{(n)}}{\partial \Delta L_b}>0 \Leftarrow E<V_b\,. \tag{44}$$

Therefore $(B^{1/2}AB^{1/2})^n$-SL's $[(BA)^n$-SL's] show the shortest (longest) in-resonance tunneling times of all $(B^{1-\gamma}AB^{\gamma})^n$-SL's.

VII. CONCLUSIONS

We have shown that coherent transport in periodic structures can be very easily optimized or tuned. The integrated transmission through minibands below the potential of the barriers can be increased, while the resonance energies and therefore the position of the minibands do not change. Applied to superlattices (SL's) the modification of only two barrier layer thicknesses allows the tuning the transmission of SL minibands in a wide range. The maximum increase of the transmission is reached for the case of a symmetric antireflection coating (ARC), consisting of one barrier with half the width of the SL barriers on each side of the SL. The ratio of the integrated transmission through normal SL minibands and the miniband width drops exponentially with the barrier width. For the SL with ARC this ratio is constant. Therefore for thick barriers the application of the ARC results in a strong increase of the integrated transmission (a factor of more than 100, for the parameters which we studied). Calculations of the in-resonance phase tunneling time show a faster tunneling process in the SL with ARC. All properties were shown to be valid for any number of periods n.

ACKNOWLEDGMENTS

C. Pacher is grateful to W. Boxleitner for fruitful discussions. We acknowledge support by the Austrian Science Fonds (FWF) Grant No. Z24.

APPENDIX A: DEFINITIONS AND IDENTITIES

The transfer matrix M_A of a well of width L_w is given by

$$M_A=\mathrm{diag}[\exp(-ikL_w);\exp(ikL_w)]. \tag{A1}$$

The elements of the transfer matrix M_B of a barrier are given by

$$\begin{aligned} a_B&=\cosh\kappa L_b-ic_2\sinh\kappa L_b\,,\\ b_B&=ic_1\sinh\kappa L_b=iA(L_b). \end{aligned} \tag{A2}$$

The elements of the transfer matrix $M_{SL}^{(1)}=M_BM_A$ of one period of a superlattice are given by

$$\begin{aligned} a_{\mathrm{SL}}^{(1)}&=P(L_b)+iS(L_b),\\ b_{\mathrm{SL}}^{(1)}&=iA(L_b)\exp ikL_w\,, \end{aligned} \tag{A3}$$

where

$$S(L_b)=\mathrm{Im}\{a_{\mathrm{SL}}^{(1)}\}=-\cosh\kappa L_b\sin kL_w-c_2\sinh\kappa L_b\cos kL_w\,, \tag{A4}$$

and $A(L_b)$ and $P(L_b)$ are defined by Eqs. (21) and (22), respectively.

The imaginary part of a_{B1AB2} reads

$$\begin{aligned} \mathrm{Im}\{a_{B1AB2}\}&=\mathrm{Im}\{a_{\mathrm{SL}}^{(1)}\}+2A(L_{b1})A(L_{b2})\sin kL_w\\ &=S(L_b)+c_1^2(\cosh\kappa L_b-\cosh\kappa\Delta L_b)\sin kL_w\,, \end{aligned} \tag{A5}$$

where $\Delta L_b=L_{b1}-L_{b2}$.

APPENDIX B: PROOF TO SEC. IV C

To prove that $|b_{B1AB2}|^2$ decreases monotonic with decreasing ΔL_b, we show that $d(|b_{B1AB2}|^2)/d\Delta L_b>0$ for $\Delta L_b>0$ and $d(|b_{B1AB2}|^2)/d\Delta L_b=0$ for $\Delta L_b=0$ (ΔL_b is re-

stricted to positive values). The following definition and identity will be used:

$$Q(L_b) := \sinh \kappa L_b \cos kL_w - c_2 \cosh \kappa L_b \sin kL_w ,$$
$$P^2(L_b) - Q^2(L_b) = 1 - c_1^2 \sin^2 kL_w . \tag{B1}$$

The calculation of the first derivative of $|b_{B1AB2}|^2$ with respect to ΔL_b yields

$$\begin{aligned} d(|b_{B1AB2}|^2)/d\Delta L_b &= d(\mathrm{Im}^2\{a_{B1AB2}\})/d\Delta L_b \\ &= 2c_1^2 \kappa \sinh \kappa \Delta L_b [Q(L_b) c_2 \sin kL_w \\ &\quad + c_1^2 \sin^2 kL_w \cosh \kappa \Delta L_b]. \end{aligned} \tag{B2}$$

The condition $P^2(L_b) \leqslant 1$ inside a miniband leads together with Eq. (B1) to

$$Q(L_b)^2 \leqslant c_1^2 \sin^2 kL_w \Leftrightarrow |Q(L_b)| \leqslant |c_1 \sin kL_w| . \tag{B3}$$

From Eqs. (B3) and the identity $c_1^2 - c_2^2 = 1$ we obtain

$$Q(L_b) c_2 \sin kL_w + c_1^2 \sin^2 kL_w > 0. \tag{B4}$$

If we consider only energies $E < V_b$, the decaying wave vector κ, defined in Table I, is a real positive number, $\cosh(\kappa \Delta L_b) \geqslant 1$ and we therefore get

$$Q(L_b) c_2 \sin kL_w + c_1^2 \sin^2 kL_w \cosh \kappa \Delta L_b > 0. \tag{B5}$$

Substituting Eq. (B5) into Eq. (B2) completes the proof. Note that the transmission does not depend on ΔL_b for energies where $\sin kL_w = 0$ is fulfilled.

It is important to notice that this proof fails for energies $E > V_b$, since κ becomes imaginary, therefore $\cosh(\kappa L_b) \leqslant 1$. Now Eq. (B5) cannot be deduced from Eq. (B4) and does not hold any longer. Indeed for energies above the barriers the transmission through the normal superlattice can be higher than the transmission through the superlattice with ARC [Fig. 2(c)].

[1] F. Capasso, Science **235**, 172 (1987).
[2] G. Bastard, Phys. Rev. B **24**, 5693 (1981).
[3] G. Bastard, Phys. Rev. B **25**, 7584 (1982).
[4] S.R. White and L.J. Sham, Phys. Rev. Lett. **47**, 879 (1981).
[5] M. Altarelli, Phys. Rev. B **28**, 842 (1983).
[6] E.O. Kane, *Tunneling Phenomena in Solids*, edited by E. Burnstein and S. Lundquist (Plenum Press, New York, 1969).
[7] B. Ricco and M.Ya. Azbel, Phys. Rev. B **29**, 1970 (1984).
[8] L. Esaki and R. Tsu, IBM J. Res. Dev. **14**, 61 (1970).
[9] M. Pacheco and F. Claro, Phys. Status Solidi B **114**, 399 (1982).
[10] D.J. Vezetti and M. Cahay, J. Phys. D **19**, L53 (1986).
[11] H. Yamamoto, Y. Kanie, and K. Taniguchi, Phys. Status Solidi B **154**, 195 (1989).
[12] D.W.L. Sprung, H. Wu, and J. Martorell, Am. J. Phys. **61**, 1118 (1993).
[13] P. Pereyra and E. Castillo, Phys. Rev. B **65**, 205120 (2002).
[14] D.J. Griffiths and N.F. Taussig, Am. J. Phys. **60**, 883 (1992).
[15] To prevent some possible confusion we note that the transfer matrix can be also defined by $(A_R^+, A_R^-)^T = \hat{M}(A_L^+, A_L^-)^T$, for the example used in Ref. 13. Of course, $\hat{M} = M^{-1}$. The reader is asked to check carefully which definition is used when he consults the literature, since both occur frequently.
[16] C. Pacher, C. Rauch, G. Strasser, E. Gornik, F. Elsholz, A. Wacker, G. Kießlich, and E. Schöll, Appl. Phys. Lett. **79**, 1486 (2001).
[17] P. Erdös and R.C. Herndon, Adv. Phys. **31**, 65 (1982).
[18] M. Born and E. Wolf, *Principles of Optics*, 6th ed (Pergamon Press, Oxford, 1980), p. 67.
[19] M. Abramovitz and I.A. Stegun, *Handbook of Mathematical Functions* (Dover, New York, 1967).
[20] P.F. Yuh and K.L. Wang, Phys. Rev. B **38**, 13 307 (1988).
[21] P. Pereyra, Phys. Rev. Lett. **84**, 1772 (2000).
[22] While transforming the potential, new transmission resonances can occur, or transmission resonances can vanish (e.g., while transforming a period consisting of a simple barrier/well pair in a barrier/well/barrier structure and vice versa), but these transmission resonances belong to the single period of the potential and are not due to the periodicity.
[23] An energy-dependent effective mass $m(E)$ to include nonparabolicity of the conduction band can simply be used by replacing each occurrence of m in all formulas with $m(E)$.